ORIGINAL PAPER

Structure Types of Kidney Stones and Their Susceptibility to Shock Wave Fragmentation

Sergiy Kolupayev[1,2], Vladimir Lesovoy[1], Elena Bereznyak[3], Nina Andonieva[1], Dmytro Shchukin[1]

[1]Department of Urology, Nephrology and Andrology, Kharkiv National Medical University, Kharkiv, Ukraine

[2]Department of Minimally Invasive Treatment, V.I. Shapoval Regional Medical Clinical Center of Urology and Nephrology, Kharkiv, Ukraine

[3]Institute of Solid-State Physics, Materials Science and Technologies, National Science Center Kharkiv Institute of Physics and Technology, Kharkiv, Ukraine

Corresponding author: Sergiy Kolupayev, MD, PhD, Department of Urology, Nephrology and Andrology, Kharkiv National Medical University. Address: 195 Moskovskyy Avenue, Kharkiv 61037, Ukraine. Fax/Phone: +380577387155. E-mail address: sm_kolupayev@ukr.net. **ORCID ID: https://orcid.org/0000-0001-7128-4555.**

doi: 10.5455/aim.2021.29.26-31

ACTA INFORM MED. 2021 MAR 29(1): 26-31

Received: Jan 05, 2021

Accepted: Mar 10, 2021

ABSTRACT

Background: The modern approach in the treatment of urolithiasis involves the use of non-invasive and minimally invasive techniques based on the stone fragmentation, among which shock wave lithotripsy (SWL) is considered as the first-line treatment for kidney stones < 2 cm and proximal ureter stones. **Objective:** To study the microstructure and mineral composition of kidney stones and to evaluate their influence on the stones' susceptibility to fragmentation by shock waves. **Methods:** The microstructure and mineral composition of kidney stone samples obtained from shock wave lithotripsy in 87 patients were studied using crystal optical analysis and infrared spectroscopy. The volume fraction of amorphous and crystalline phases of the stone composition, the quantitative and qualitative composition of mineral components were assessed. The fragmentation features of stones with different microstructure were retrospectively analyzed based on the total number of shock waves required for complete stone fragmentation. **Results:** Three kidney stone structure types were identified: amorphous-crystalline structure stones predominantly including the amorphous phase (type A); amorphous-crystalline structure stones predominantly including the crystalline phase (type B); fully crystalline structure stones (type C). Significant positive correlation between the total number of shock waves required for complete stone fragmentation and the volume fraction of crystalline phase was found. **Conclusion:** The structure type of kidney stones is determined by the volume ratio between the amorphous and crystalline phases of their composition. The amorphous-crystalline structure stones with the predominant content of the amorphous phase are more sensitive to shock-wave exposure. The increase in the volume fraction of crystalline phase in the stone structure reduces the stone's susceptibility to fragmentation by shock waves.

Keywords: amorphous phase, crystal optical analysis, crystalline phase, kidney stone, microstructure, shock wave lithotripsy.

1. BACKGROUND

Urolithiasis takes a leading place in the structure of urological diseases. Its prevalence in the modern population, according to various epidemiological studies, is 5-13%, depending on the region (1-3). The modern approach in the treatment of urolithiasis involves the use of non-invasive and minimally invasive techniques based on the stone fragmentation, among which shock wave lithotripsy (SWL) is considered as the first-line treatment for kidney stones < 2 cm and proximal ureter stones (4-6).

One of the factors influencing the effectiveness of SWL is the mineral composition of the stone (7, 8).

However, there are studies reporting that stones with the same mineral composition have different character of fragmentation when exposed to shock waves (9, 10). The possible cause of this phenomenon may be the special features of stones determined by a variable structural state of their mineral components.

2. OBJECTIVE

In this work, we have studied the microstructure and mineral composition of kidney stones, as well as their predisposition to fragmentation by shock waves.

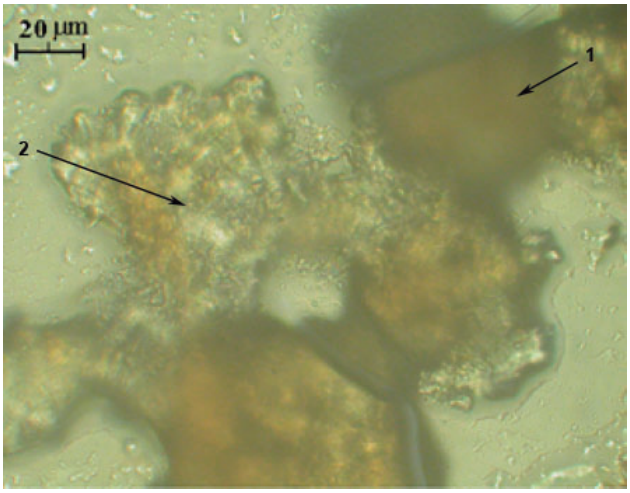

Figure 1. An immersion photomicrograph of a kidney stone specimen under transmitted light. The main amorphous mass in the form of irregular clusters of grayish-brown color with blurred edges and 30-100 μm in size (1), in which the crystalline phase is recognized, presented as a grayish-yellow translucent fine crystalline mass (2).

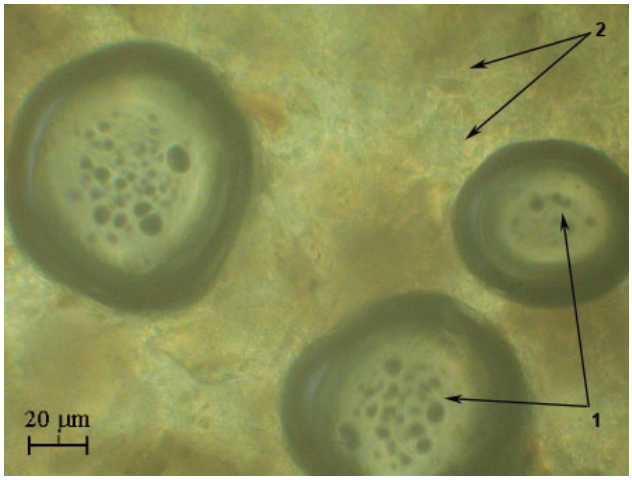

Figure 2. An immersion photomicrograph of a kidney stone specimen under transmitted light. Large (40-60 μm) spherical crystallization nuclei of whewellite (1) among the fine crystalline phosphate mass (2).

3. MATERIALS AND METHODS

We have studied the microstructure and mineral composition of kidney stone fragments obtained from 87 patients (27 females, 60 males) aged 26-63 years (average age 41.08±8.62) with solitary renal stones after SWL done with Dornier Compact Sigma Lithotripter (Dornier Medtech, Germany) at V. I. Shapoval Regional Medical Clinical Center of Urology and Nephrology, Kharkiv, Ukraine.

The stone microstructure was assessed by the method of crystal optical analysis in conjunction with immersion liquids using the polarizing microscope Polam 211L, LOMO (Russia).

With the use of the eyepiece graticule, based on the principles of quantitative analysis of microscopic images (11), the quantitative parameters of the amorphous and crystalline phases of the stone composition such as volume fraction of the amorphous phase (VFAP) and volume fraction of the crystalline phase (VFCP) were calculated. The linear dimensions, shape, color, and transparency level of the crystalline elements were also assessed.

The stone mineral composition was measured by infrared (IR) spectroscopy method using the IR spectrometer IRS-29 (LOMO, Russia) with the spectral range of 4000-400 cm^{-1}. Powdered samples obtained by grinding the fragments of urinary tract stones in agate mortars to a particle size of ~ 1-10 μm were studied. The samples were prepared from a mixture of potassium bromide as a matrix (99%) and the test substance (1%). A 100-mg aliquot of the resulting homogenized powder was then pressed into a transparent pellet. To exclude the matrix absorption bands, a pure potassium bromide pellet, preliminarily dried at 180°C during 10 hours, was placed in the sample compartment of the device.

The calibration was performed according to the spectrum of polystyrene with known frequencies of absorption maxima. The adjustment averaged 5 to 10 cm^{-1}. The mineral composition of the stone was evaluated based on the identification of the infrared absorption bands which were specific to certain chemical compounds (12, 13). The intensity of the absorption bands, the characteristics of the maxima, and the transmission level were also determined.

At the final stage of the study, the initial parameters and susceptibility to shock wave fragmentation of stones with different structural features were assessed based on the retrospective analysis of the patients' medical records. The initial stone parameters were determined using non-contrast computed tomography (NCCT) with Toshiba Aquilion 16 CT scanner (Japan), performed in all patients before SWL. The maximum stone length (MSL) and mean stone density (MSD) were assessed. The maximum linear size of the stone in the axial or coronal plane was considered as the MSL (14). The MSD was calculated as the mean density index in Hounsfield units, measured in the plane where the elliptical region of interest included the largest cross-sectional area of the stone, excluding adjacent soft tissue (15). The stone susceptibility to shock wave fragmentation was assessed by the total number of shock waves (SWs) during all lithotripsy sessions required for complete stone fragmentation and achieving the "stone free" status meaning absolute clearance or residual stone fragments less than 4 mm according to the NCCT confirmation at the end of treatment.

Statistical data processing was performed using Microsoft Excel 2016 spreadsheets and Statistica 10 (StatSoft, USA). An intergroup comparison of three independent samples was performed using the Kruskal-Wallis test. The quantitative variables, that showed statistically significant differences ($p<0.05$) according to the Kraskel-Wallis criterion, were additionally analyzed using a post hoc Mann-Whitney U test.

The direction and strength of the relationship between the variables were evaluated using Spearman's correlation coefficient.

4. RESULTS

The crystal optical analysis of the urinary stone samples revealed the presence of amorphous and crystalline phases, either isolated or combined with each other.

The amorphous phase, when observed in an immersion preparation, presented as a translucent or opaque mass, composed by grayish-brown clusters of an irregular shape with indistinct edges, of 30-120 μm in size (Figure

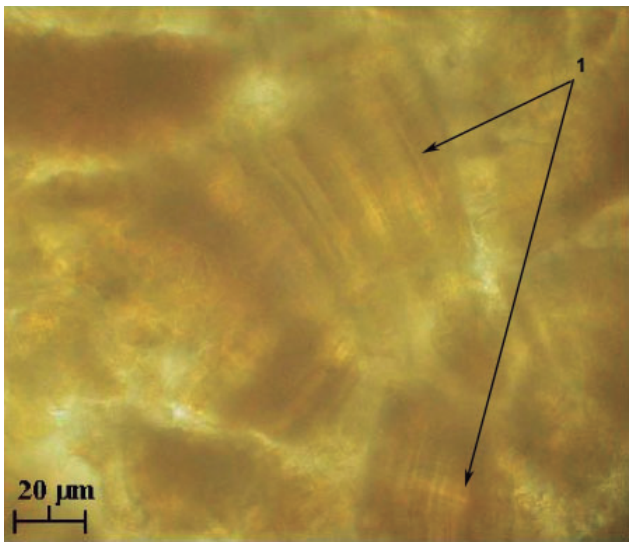

Figure 3. An immersion photomicrograph of a kidney stone specimen under transmitted light. Transparent grains of crystalline whewellite from light-yellow to bright-orange color with characteristic streaked texture (1).

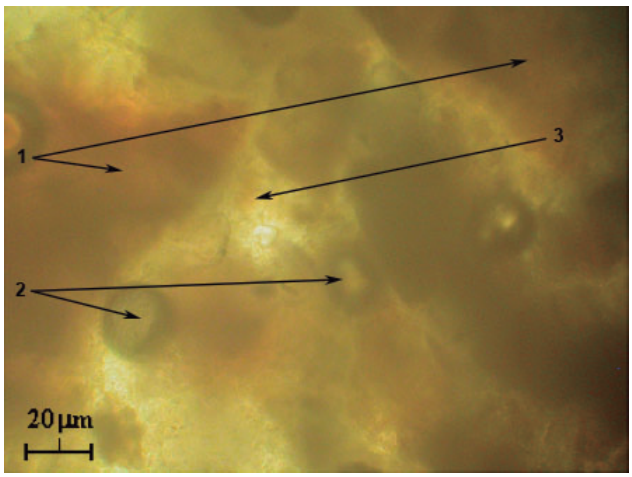

Figure 4. An immersion photomicrograph of a kidney stone specimen under transmitted light. Structure type A: an amorphous-crystalline structure of the stone, predominantly in the amorphous phase represented by whewellite (1), with multiple small (5-20 µm) crystallization nuclei (2) and a gray fine crystalline mass consisting of calcium phosphates (3). VFCP ~ 40 vol%.

1).

The crystalline phase was characterized by various structural elements corresponding to different evolutionary stages of crystal formation: globules of 10-50 µm in size with dark edges and transparent crystalline substance in the center (crystallization nuclei) (Figure 2); transparent, translucent and opaque grains of 20-80 µm with various color intensity, from light-beige to black (Figure 3).

According to the quantitative ratio between the amorphous and crystalline phases of the stone structure, as well as the available data on the evolutionary principles of biominerals formation involving the consecutive crystallization of the amorphous phase (16-18), three structure types of kidney stones were distinguished.

Structure type A: an amorphous-crystalline structure with the predominant amorphous phase (VFAP > 50 vol%). The crystalline phase was formed of crystalline nuclei and fine crystalline mass (up to 30 µm) without clear differentiation (Figure 4).

Structure type B: an amorphous-crystalline structure with the predominant crystalline phase (VFCP > 50 vol%). The fine crystalline mass was formed of crystal grains of varying transparency (Figure 5).

Structure type C: a crystalline structure without the amorphous phase. The fully crystalline phase (VFCP = 100 vol%) was formed of crystals in the shape of grains with the structural characteristics depending on the mineral type (Figure 6).

Out of all 87 samples analyzed, structure type A, B and C stones were identified in 22 (25.29%), 39 (44.83%) and 26 (29.88%) patients, respectively.

Infrared spectroscopy of various structure type stones revealed a wide range of chemical compounds. The most common chemical compounds were calcium oxalate (CaOx) in the form of whewellite (calcium oxalate monohydrate) or weddellite (calcium oxalate dihydrate), cal-

Number of mineral components	Qualitative mineral composition of the stone	Structure type A n=22	Structure type B n=39	Structure type C n=26
1 component, n=21	CaOx	3 (13.64%)	4 (10.26%)	4 (15.38%)
	Uric acid	2 (9.09%)	4 (10.26%)	3 (11.54%)
	Ammonium urate	0	1 (2.56%)	0
2 components, n=52	CaOx + CaP	12 (54.54%)	20 (51.28%)	11 (42.31%)
	CaOx + uric acid	2 (9.09%)	4 (10.26%)	3 (11.54%)
3 components, n=14	CaOx + Ca carbonate + uric acid	0	0	1 (3.85%)
	CaOx+ CaP + uric acid	3 (13.64%)	5 (12.82%)	4 (15.38%)
	Uric acid + CaP + aragonite	0	1 (2.56%)	0

Table 1. Quantitative and qualitative characteristics of the stone structure types

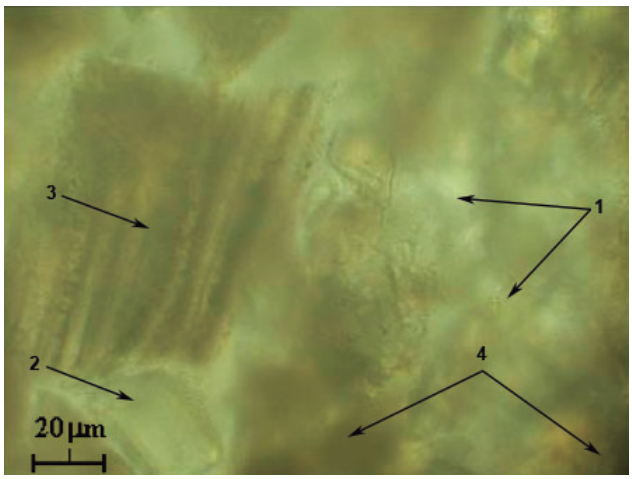

Figure 5. An immersion photomicrograph of a kidney stone specimen under transmitted light. Structure type B: an amorphous-crystalline structure of the stone, predominantly in the crystalline phase, represented by whewellite in the form of a fine crystalline mass (1), formed transparent grains (2) and grains with characteristic streaked texture (3) against the background of an amorphous phosphate mass (4). VFCP ~ 80 vol%.

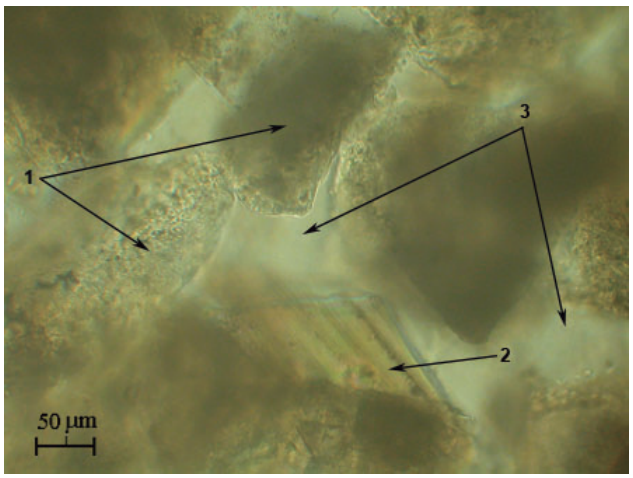

Figure 6. An immersion photomicrograph of a kidney stone specimen under transmitted light. Structure type C: a crystalline structure represented by large (100-250 µm) transparent and translucent grains of gray apatite (1), among which grains of whewellite with characteristic streaked texture (2) and a fine crystalline mass of calcium phosphate can be encountered (3). VFCP = 100 vol%.

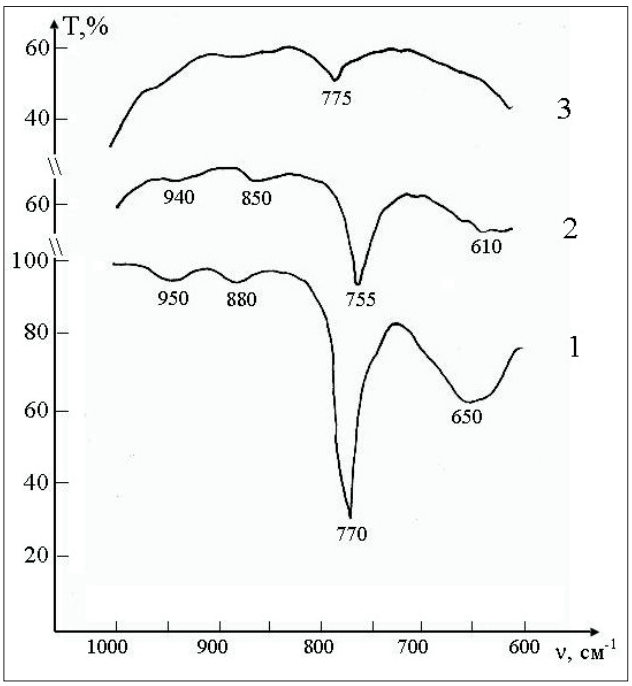

Figure 7. IR spectra of amorphous, amorphous-crystalline and crystalline whewellite in the range of 600-1000 cm^{-1}. Curve 1–crystalline whewellite; Curve 2–amorphous-crystalline whewellite (VFAP~ 30 vol%); Curve 3–amorphous whewellite.

cium phosphates (CaP) in the form of apatite, hydroxylapatite, fluorapatite, and uric acid. Aragonite, calcium carbonate, and ammonium urate were identified in rare cases. Sixty-six (75.86%) stones had a mixed mineral composition with two or more components (Table 1).

The appearance of the IR spectrum was dependent on the structural state of the minerals composing the stone. The amorphous phase was characterized by absorption bands of low and medium intensity, often with wide or blurred maxima and low transmittance (T=30-50%). The spectral properties of the crystalline phase were the increased number of characteristic absorption bands of medium and high intensity with narrow maxima, as well as high transmittance (T=70-80%) (Figure 7).

Despite the qualitative differences between the IR spectra of the amorphous and crystalline phases, it was not possible to measure their quantity in the stone sample and to determine the stone structure type by the spectral curve pattern.

The features of the kidney stone structure types were evaluated based on the tomographic parameters (MSL, MSD), as well as SWs number characterizing the stone susceptibility to shock wave fragmentation. Comparative analysis of various structure types of kidney stones revealed statistically significant differences in SWs between the study groups. The maximum values of this parameter was observed in the group of patients with structure type C stones. No significant difference between MSL and MSD parameters was seen in the stone samples of different structure types (p>0.05) (Table 2).

Taking into account the VFCP increase from stone structure type A through stone structure type C, a correlation analysis was performed between the VFCP and SWs parameters. A positive statistically significant correlation (p<0.05; r=0.49) between these parameters was revealed, i.e. the increase in the quantity of the crystalline phase of the stone composition required the increased number of shock waves to fulfil the complete fragmentation and achieve "stone free" status.

Parameters	Type A	Type B	Type C	P-value*
	Me [Q1-Q3]	Me [Q1-Q3]	Me [Q1-Q3]	
MSD (HU)	1274.50 [1161.00-1358.75]	1259.00 [814.00-1685.00]	1466.50 [1241.50-1546.75]	0.13
MSL (mm)	14.05 [11.23-15.18]	11.00 [9.50-14.00]	12.00 [9.63-14.38]	0.094
SWs	2990.00 [2675.00-4115.00]	4200.00† [3135.00-5285.00]	5025.00†‡ [3770.50-7907.50]	<0.01

Table 2. Comparative analysis of kidney stone structure types Me–median; MSD – mean stone density; MSL – maximum stone length; HU–Hounsfield Units; [Q1-Q3]–interquartile range; SWs–total number of shock waves required for complete stone fragmentation. *–Kruskal-Wallis test; †–significant difference (p<0.01) compared to type A (post hoc analysis using Mann-Whitney U test); ‡–significant difference (p<0.01) compared to type B (post hoc analysis using Mann-Whitney U test).

5. DISCUSSION

The current trend in the management of urolithiasis is the use of various types of lithotripsy, among which SWL remains relevant and continues to be considered as the first-line treatment in most patients with kidney and ureter stones (19-21). Among the factors influencing the outcomes of SWL, the composition- and structure-dependent fragility of a calculus appears to be of great importance (7, 22, 23). Therefore, the adequate analysis of a kidney stone should involve a comprehensive assessment of its mineral composition and internal structure. Currently, the IR spectroscopy and X-ray diffraction are widely used as the methods for evaluating the mineral composition of a stone (24-26). However, these methods do not allow us to make a comprehensive assessment of the calculus structural features.

It is reported that the synchrotron radiation microtomography (SR-µCT) is used for evaluation of the micro-

structure and mineral composition of kidney stones. However, this method cannot be easily applied to the routine practice, and is only appropriate in the study of rare, non-typical samples (27).

In our work, the stone microstructure was assessed by crystal optical analysis using a polarizing microscope with immersion liquids. Polarization microscopy as a method for analyzing kidney stones has been used by a number of authors to evaluate the stone mineral composition (28, 29). However, the accuracy of component identification in the mixed combinations, especially those containing uric acid, calcium phosphate and purine derivatives, is inferior to spectroscopic methods (29), which is why it has not been widely used in the urolithiasis diagnosis. The use of polarizing microscopy is more reasonable in cases of assessment of the volume fraction of the crystalline and amorphous phases. The advantages of this method are its economic efficiency, speed of execution, and the ability to use a small amount of substance (30).

According to modern concepts, the crystallization process passes through the amorphous phase (16-18). In 70.1% of our patients, the amorphous phase in the structure of the urinary stone was present along with the crystalline phase, which was a sign of an incomplete crystallization process, suggesting a relatively young age of a stone. The ratio of the crystalline and amorphous phases of the calculus structure is both characteristic of the temporal parameters of stone formation, and also is a factor determining the degree of stone predisposition to fragmentation by shock waves.

The results of our study show that the stone structure types with a higher level of the VFAP and immature crystalline forms are better disintegrated by SWL, allowing us to consider the stone structure type as the factor impacting the effectiveness of SWL. Further research in the field of urolithiasis diagnosis is apparently needed to find the visual criteria for distinguishing the structure types of urinary stones, which will be the basis for a differentiated approach to choosing a treatment option in different patients.

Based on the data of the crystal optical analysis, the renal stones, according to their structural state depending on the volume ratio between the amorphous and crystalline phases can be divided into three types: structure type A, which are the amorphous-crystalline structure stones with the predominant content of the amorphous phase (> 50 vol%); structure type B, which are the amorphous-crystalline structure stones with the predominant content of the crystalline phase (> 50 vol%); structure type C, which are the stones with fully crystalline structure. The presence of the amorphous phase, as well as immature crystalline forms, indicates an incomplete crystallization process and makes the stone more susceptible to shock wave exposition. The increased VFCP of the stone structure reduces its susceptibility to shock wave fragmentation. Determining the structure type of a stone by crystal optical analysis is a reasonable component of a complex assessment of kidney stones.

6. CONCLUSION

The structure type of kidney stones is determined by the volume ratio between the amorphous and crystalline phases of their composition. The amorphous-crystalline structure stones with the predominant content of the amorphous phase are more sensitive to shock-wave exposure. The increase in the volume fraction of crystalline phase in the stone structure reduces the stone's susceptibility to fragmentation by shock waves.

- **Patient Consent Form:** The study was performed in accordance with the principles of Declaration of Helsinki and approved by the Ethics Committee of V.I. Shapoval Regional Clinical Centre of Urology and Nephrology. The participants were informed about the aim, methods and design of the study and provided the written informed consent.
- **Author's contribution:** All authors were involved in the preparation of this manuscript. Final proofreading was made by the first author.
- **Conflict of interest:** None declared.
- **Financial support and sponsorship:** None.

REFERENCES

1. Alatab S, Pourmand G, El Howairis Mel F, Buchholz N, Najafi I, Pourmand MR. et al. National profiles of urinary calculi: a comparison between developing and developed worlds. Iran J Kidney Dis. 2016; 10: 51-61.
2. Ahmad F, Nada MO, Farid AB, Haleem MA, Razack S. Epidemiology of urolithiasis with emphasis on ultrasound detection: a retrospective analysis of 5371 cases in Saudi Arabia. Saudi J Kidney Dis Transpl. 2015; 26: 386-391; https://doi.org/10.4103/1319-2442.152557.
3. Sorokin I, Mamoulakis C, Miyazawa K, Rodgers A, Talati J, Lotan Y. Epidemiology of stone disease across the world. World J Urol. 2017; 35: 1301-1320; https://doi.org/10.1007/s00345-017-2008-6.
4. Al-Marhoon MS, Shareef O, Al-Habsi IS, Al Balushi AS, Mathew J, Venkiteswaran KP. Extracorporeal shock-wave lithotripsy success rate and complications: initial experience at Sultan Qaboos University Hospital. Oman Med J. 2013; 28: 255-259; https://doi.org/10.5001/omj.2013.72.
5. Turk C, Neisius A, Petřík A, Seitz C, Skolarikos A, Thomas K. et al. EAU Guidelines on Urolithiasis 2020. Edn. presented at the EAU Annual Congress Amsterdam 2020. ISBN 978-94-92671-07-3. Publisher: The European Association of Urology Guidelines Office. Place published: Arnhem, The Netherlands. Available from: https://uroweb.org/guideline/urolithiasis.
6. Badawy AA, Saleem MD, Abolyosr A, Aldahshoury M, Elbadry MSB, Abdalla MA. et al. Extracorporeal shock wave lithotripsy as first line treatment for urinary tract stones in children: outcome of 500 cases. Int Urol Nephrol. 2012; 44: 661-666; https://doi.org/10.1007/s11255-012-0133-0.
7. Kijvikai K, de la Rosette JJM. Assessment of stone composition in the management of urinary stones. Nat Rev Urol. 2011; 8: 81-85; https://doi.org/10.1038/nrurol.2010.209.
8. Nasef AS, El-Feky MM, El-Shorbagy MS, Elzayat TM, Elguoshy FI. The relationship between renal stone radio-density, chemical composition, and fragmentation by extracorporeal shock-wave lithotripsy. Al-Azhar Assiut medical Journal. 2015; 13: 63-68.
9. Williams JC Jr, Saw KC, Paterson RF, Hatt EK, McAteer JA, Lingeman JE. Variability of renal stone fragility in shock wave lithotripsy. Urology. 2003; 61: 1092-1096; https://doi.org/10.1016/

S0090-4295(03)00349-2.

10. Daudon M, Bazin D, Andre G, Jungers P, Cousson A, Chevallier P. et al. Examination of whewellite kidney stones by scanning electron microscopy and powder neutron diffraction techniques. J Appl Crystallogr. 2009; 42: 109-115; https://doi.org/10.1107/S0021889808041277.
11. James J, Tanke HJ. Biomedical Light Microscopy. Springer, Dordrecht, 1991; https://doi.org/10.1007/978-94-011-3778-2.
12. Ma RH, Luo XB, Li Q, Zhong HQ. The systematic classification of urinary stones combine-using FTIR and SEM-EDAX. Int J Surg. 2017; 41: 150-161; https://doi.org/10.1016/j.ijsu.2017.03.080.
13. Sekkoum K, Abdelkrim C, Taleb S, Belboukhari N. FTIR spectroscopic study of human urinary stones from El Bayadh district (Algeria). Arabian journal of chemistry. 2016; 9: 330-334; https://doi.org/10.1016/j.arabjc.2011.10.010.
14. Kim JC, Cho KS, Kim DK, Chung DY, Jung HD, Lee JY. Predictors of uric acid stones: mean stone density, stone heterogeneity index, and variation coefficient of stone density by single-energy non-contrast computed tomography and urinary pH. J Clin Med. 2019; 8: 243; https://doi.org/10.3390/jcm8020243.
15. Chung DY, Cho KS, Lee DH, Han JH, Kang DH, Jung HD. et al. Impact of colic pain as a significant factor for predicting the stone free rate of one-session shock wave lithotripsy for treating ureter stones: a Bayesian logistic regression model analysis. PLoS ONE. 2015; 10: e0123800; https://doi.org/10.1371/journal.pone.0123800.
16. Prywer J, Mielniczek-Brzoska E. Formation of poorly crystalline and amorphous precipitate, a component of infectious urinary stones: role of tetrasodium pyrophosphate. Cryst Growth Des. 2019; 19: 1048-1056; https://doi.org/10.1021/acs.cgd.8b01581.
17. Gower LB. Biomimetic model systems for investigating the amorphous precursor pathway and its role in biomineralization. Chem. Rev. 2008; 108: 4551-4627; https://doi.org/10.1021/cr800443h.
18. Ihli J, Wang YW, Cantaert B, Kim YY, Green DC, Bomans PHH. et al. Precipitation of amorphous calcium oxalate in aqueous solution. Chem Mater. 2015; 27: 3999-4007; https://doi.org/10.1021/acs.chemmater.5b01642.
19. Lawler AC, Ghiraldi EM, Tong C, Friedlander JI. Extracorporeal Shock Wave Therapy: Current Perspectives and Future Directions. Curr Urol Rep. 2017; 18: 25; https://doi.org/10.1007/s11934-017-0672-0.
20. Desai M, Sun Y, Buchholz N, Fuller A, Matsuda T, Matlaga B. et al. Treatment selection for urolithiasis: percutaneous nephrolithomy, ureteroscopy, shock wave lithotripsy, and active monitoring. World J Urol. 2017; 35: 1395-1399; https://doi.org/10.1007/s00345-017-2030-8.
21. Neisius A, Lipkin ME, Rassweiler JJ, Zhong P, Preminger GM, Knoll T. Shock wave lithotripsy: the new phoenix? World J Urol. 2015; 33: 213-221; https://doi.org/10.1007/s00345-014-1369-3.
22. Taton G, Rokita E, Wrobel A, Beckmann F, Thor P, Worek M. Analysis of renal calculi structure with the use of X-ray microtomography. In: Dossel O, Schlegel WC. (eds): World Congress on Medical Physics and Biomedical Engineering, September 7-12, 2009, Munich, Germany. IFMBE Proceedings, vol 25/4. Springer, Berlin, Heidelberg. 2009; https://doi.org/10.1007/978-3-642-03882-2_101.
23. Pittomvils G, Vandeursen H, Wevers M, Lafaut JP, De Ridder D, De Meester P. et al. The influence of internal stone structure upon the fracture behaviour of urinary calculi. Ultrasound Med Biol. 1994; 20: 803-810; https://doi.org/10.1016/0301-5629(94)90037-X.
24. Kravdal G, Helgo D, Moe MK. Infrared spectroscopy is the gold standard for kidney stone analysis. Tidsskr. Nor. Laegeforen. 2015; 135: 313-314; https://doi.org/10.4045/tidsskr.15.0056.
25. Popescu (Pintilie) GS, Ionescu I, Grecu R, Preda A. The use of infrared spectroscopy in the investigation of urolithiasis. Rev Rom Med Lab. 2010; 18: 67-77; http://www.rrml.ro/articole/articol.php?year=2010&vol=4&poz=8.
26. Yapanoğlu T, Demirel A, Adanur Ş, Yüksel H, Polat Ö. X-ray diffraction analysis of urinary tract stones. Turk J Med Sci. 2010; 40: 415-420; doi:10.3906/sag-0909-270.
27. Kaiser J, Hola M, Galiova M, Novotny K, Kanicky V, Martinec P. et al. Investigation of the microstructure and mineralogical composition of urinary calculi fragments by synchrotron radiation X-ray microtomography: a feasibility study. Urol Res. 2011; 39: 259-267; https://doi.org/10.1007/s00240-010-0343-9.
28. Douglas DE, Tonks DB. The qualitative analysis of renal calculi with the polarising microscope. Clinical biochemistry. 1979; 12: 182-183; https://doi.org/10.1016/S0009-9120(79)80086-7.
29. Basiri A, Taheri M, Taheri F. What is the state of the stone analysis techniques in urolithiasis? Urol J. 2012; 9: 445-454.
30. Singh VK, Rai PK. Kidney stone analysis techniques and the role of major and trace elements on their pathogenesis: a review. Biophys Rev. 2014; 6: 291-310. https://doi.org/10.1007/s12551-014-0144-4.